Effect of Passivation Time on the Corrosion Resistance of 6005A Aluminum Alloy

Author：KaiBo Yang, KeJun Jiang

Abstract—

To enhance the corrosion resistance of 6005A aluminum alloy in chloride-containing environments, chemical passivation was conducted in a 1 mol/L sulfuric acid solution for varying durations. The influence of passivation time on the corrosion behavior was systematically investigated using potentiodynamic polarization and electrochemical impedance spectroscopy (EIS). Experimental results revealed that passivation time significantly affects the compactness and stability of the passive film, exhibiting a trend of *initial improvement followed by deterioration* in corrosion resistance. When the passivation time was 70 min, the alloy exhibited the most positive corrosion potential and pitting potential, the lowest corrosion current density, and the highest impedance modulus and phase angle peak, indicating the formation of an optimally structured passive film with superior protective performance. These findings provide both theoretical and experimental guidance for optimizing the passivation process parameters of 6005A aluminum alloy.

Index Terms— 6005A aluminum alloy; chemical passivation; passivation time; corrosion resistance; electrochemical testing

I. INTRODUCTION

A. Research Background and Significance

As a medium-strength, heat-treatable Al–Mg–Si alloy, 6005A aluminum alloy exhibits comprehensive properties that lie between those of the commonly used 6061 and 6063 alloys. After T5 or T6 heat treatment, its tensile strength typically exceeds 270 MPa, achieving a favorable balance between strength and ductility. In addition to its excellent mechanical performance, the alloy has a relatively low density of approximately 2.70 g/cm³, making it an ideal material for lightweight structural applications in fields such as rail transportation and bridge engineering.

Owing to its superior extrusion processability, good weldability, and formability, 6005A aluminum alloy is widely used in the fabrication of complex structural components, including rail vehicle frames, architectural curtain walls, bridge structures, and electronic device housings. In these applications, long-term durability and corrosion resistance are critical factors that determine the service life and reliability of the material. Although 6005A aluminum alloy can naturally form a thin passive oxide film in atmospheric environments, providing limited protection against corrosion, this naturally formed film is highly susceptible to localized breakdown by chloride ions (Cl^-) in marine atmospheres, industrially polluted regions, or environments exposed to de-icing salts. Such breakdowns often lead to severe localized corrosion forms such as pitting and crevice corrosion, which not only degrade surface aesthetics and reduce service life but also pose potential risks to structural integrity.

Therefore, improving the corrosion resistance of 6005A aluminum alloy through surface treatment techniques is of great importance. Acid passivation is a simple and cost-effective chemical surface modification method. By immersing the alloy in specific acidic media (such as sulfuric acid), the unstable natural oxide film on the surface can be removed, and a more stable, uniform, and compact chemical conversion film can be formed *in situ*, thereby significantly enhancing resistance to subsequent corrosive attacks. Among various passivation parameters, treatment time plays a critical role in determining the thickness, compactness, and chemical stability of the passive film. Insufficient passivation time may result in an incomplete film, whereas excessive time can lead to over-dissolution or structural degradation of the film—both of which compromise protective performance.

Hence, systematically investigating the influence of passivation time on the corrosion resistance of 6005A aluminum alloy and determining the optimal processing parameters are of significant theoretical and practical importance for improving the alloy’s service performance and expanding its engineering applications.

B. Research Status at Home and Abroad

At present, extensive and in-depth studies on surface protection technologies for aluminum alloys have been conducted by scholars worldwide. Among them, electrochemical methods represented by anodic oxidation are the most mature. Studies have shown that anodic oxidation in electrolytes such as sulfuric acid, oxalic acid, and phosphoric acid can generate a porous or barrier-type alumina (Al_2O_3) film on the surface of aluminum alloys, which exhibits far superior corrosion resistance compared with the naturally formed oxide film. Numerous investigations have focused on optimizing anodizing process parameters—such as electrolyte composition, temperature, current density, and voltage—to control the microstructure (e.g., pore size, wall thickness, and barrier layer thickness) and properties of the oxide film. For instance, Wang *et al.* studied the influence of current density on film properties during sulfuric acid anodizing and reported that appropriate anodizing parameters can significantly improve the corrosion resistance of aluminum alloys.

Meanwhile, chemical passivation—an electrochemically independent surface treatment technique—has also attracted continuous attention. For example, chromate-based passivation processes were once widely applied due to their excellent corrosion resistance; however, their use has been strictly restricted because of the high toxicity and environmental hazards associated with hexavalent chromium. Consequently, the development of environmentally friendly chemical conversion coating technologies has become a research hotspot, including passivation processes based on titanium/zirconium salts, rare-earth elements, and permanganates. Moutarlier *et al.* investigated the formation mechanism of cerium-based conversion films on aluminum surfaces and confirmed that cerium ions can effectively enhance resistance to chloride-induced pitting corrosion. Similarly, Peng *et al.* employed permanganate-based passivation on aluminum alloys and found that the resulting films were uniform and compact, with significantly reduced corrosion current density.

In evaluating the protective performance of passive films, electrochemical testing techniques such as potentiodynamic polarization and electrochemical impedance spectroscopy (EIS) are widely adopted. Freire *et al.* analyzed the passivation behavior of AISI 316 stainless steel in alkaline media using combined polarization and EIS tests, providing a useful reference for similar analyses in aluminum alloys. Zhao *et al.* employed EIS and Tafel analysis to study the corrosion behavior of chemically passivated aluminum alloys in 3.5% NaCl solution and found that the low-frequency impedance modulus was strongly correlated with the integrity of the passive film.

Although existing studies have provided a solid theoretical foundation for understanding the corrosion and protection mechanisms of aluminum alloys, several aspects remain insufficiently explored. Compared with complex anodizing or novel eco-friendly passivation technologies, the relatively simple sulfuric acid chemical passivation process has not been systematically studied for specific alloy grades such as 6005A, particularly regarding the quantitative relationship between passivation time—a critical process parameter—and the resulting corrosion resistance. Yang *et al.* pointed out that the formation time of the passive film directly affects both corrosion and pitting potentials, but their research mainly focused on general-purpose aluminum alloys rather than 6005A . Moreover, most studies emphasize film-formation mechanisms or comparisons with other complex processes, lacking a clear and practical “time–performance” correlation curve that could directly guide industrial production.

In this context, this study focuses on 6005A aluminum alloy and employs a 1 mol/L sulfuric acid solution for chemical passivation. By systematically varying the passivation time and applying potentiodynamic polarization and EIS techniques, the effects of passivation duration on the corrosion resistance of 6005A aluminum alloy in chloride-containing environments are comprehensively investigated. The aim is to provide reliable experimental evidence and theoretical support for optimizing the passivation parameters of this alloy.

II. EXPERIMENTAL MATERIALS AND METHODS

A. Sample Preparation

The material used in this study was commercially available 6005A aluminum alloy plate. Its main chemical composition (mass fraction, %) is as follows:

chemical component	mass fraction
Si	0.75%
Fe	0.25%
Cu	0.08%
Mn	0.45%
Mg	0.55%
Cr	0.05%
Zn	0.15%
Ti	0.08%
Al	余量

The 6005A aluminum alloy plate was cut into samples with dimensions of 10 mm × 10 mm × 10 mm using wire electrical discharge machining (EDM). A copper wire was welded to the back of each sample for electrical connection, and the specimen was then embedded in epoxy resin, leaving only one exposed surface (10 mm × 10 mm) as the working area.

To remove surface defects and the deformation layer produced during machining, the exposed surface was sequentially ground with water-abrasive silicon carbide papers of 240#, 400#, 800#, 1200#, and 1500# grit until a uniform metallic luster was obtained. The polished surface was then subjected to fine polishing using alumina suspension as the polishing agent. Subsequently, the samples were ultrasonically cleaned in deionized water and ethanol successively to obtain a clean mirror-like surface. Finally, the specimens were dried with hot air, sealed, and stored in a desiccator for subsequent experiments.

B. Solution Preparation

All chemical reagents used in this study were of analytical grade (AR), and all water used was twice-deionized water. Two types of solutions were prepared for the experiments.

The first was the chemical passivation solution, prepared by diluting concentrated sulfuric acid (H_2SO_4, 98%) with deionized water to obtain a 1 mol/L sulfuric acid solution, which was then diluted to a total volume of 2 L for standby use.

The second was the corrosion test solution, prepared by accurately weighing analytical-grade sodium chloride (NaCl) and dissolving it in deionized water to obtain a 3.5% NaCl solution, also diluted to a total volume of 2 L. This solution was used in subsequent electrochemical measurements.

C. Metallographic Observation and Analysis

The material used in this study was 6005A aluminum alloy. After standard metallographic preparation procedures—including grinding and polishing—the three-dimensional microstructure of the alloy was observed, as shown in Fig. 1.

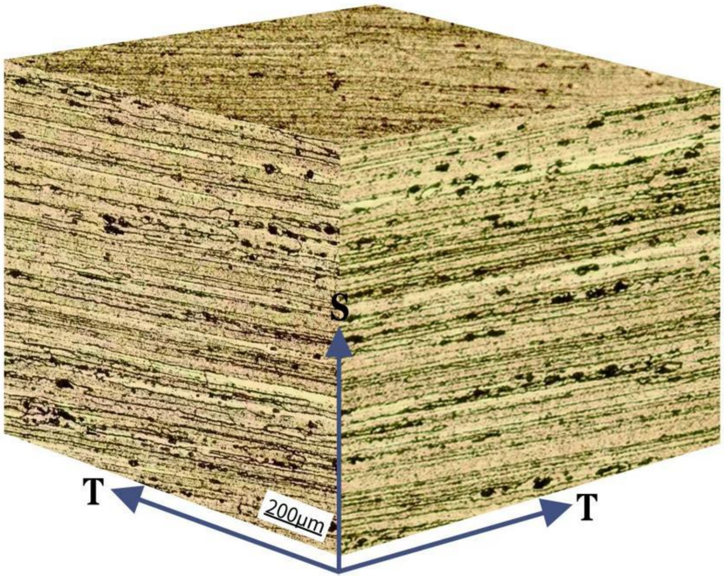

From the figure, it can be clearly seen that the alloy exhibits distinct deformation characteristics typical of a processed state. The grains are markedly elongated along a single direction, forming a fibrous and laminar structure. Numerous fine black particles are dispersed within the grains and along grain boundaries, which are generally identified as second-phase particles within the alloy. Overall, the metallographic morphology presents the typical features of a deformed aluminum alloy, and this anisotropic structure is expected to influence the alloy’s mechanical properties and subsequent surface treatment behavior.

D. Electrochemical Testing

1) Passivation Treatment

The prepared 6005A aluminum alloy specimens were immersed in a 1 mol/L sulfuric acid solution for chemical passivation. The treatment was conducted at room temperature (25 ± 2 °C), and the passivation durations were set to 10 min, 30 min, 50 min, 70 min, and 90 min, respectively. After each passivation process, the specimens were immediately removed, thoroughly rinsed with deionized water, and then immersed in a 3.5% NaCl solution to allow the electrochemical system to stabilize prior to testing.

2) Electrochemical Measurement

All electrochemical tests were conducted using a Corrtest CS-series electrochemical workstation. The corrosion medium was a 3.5 wt.% NaCl solution, and all measurements were performed at room temperature (25 ± 2 °C). A standard three-electrode configuration was employed, in which the passivated 6005A aluminum alloy specimen served as the working electrode (WE), a saturated calomel electrode (SCE) was used as the reference electrode (RE), and a large-area platinum sheet acted as the counter electrode (CE).

First, the open-circuit potential (OCP) of the passivated sample was monitored in the 3.5 wt.% NaCl solution until the potential fluctuation was less than 5 mV within 1800 s, ensuring that the electrochemical system had reached a steady state. Subsequently, electrochemical impedance spectroscopy (EIS) measurements were performed at the stabilized OCP with an AC perturbation amplitude of 10 mV. The frequency range was set from 10^5 Hz to 10^{-2} Hz.

After completing the EIS test, potentiodynamic polarization (PDP) measurements were immediately carried out. The polarization curves were scanned from −300 mV to +1000 mV relative to the OCP, with a scan rate of 1 mV/s. To ensure accuracy and reproducibility, each group of samples with different passivation durations was tested in triplicate under identical conditions.

Ⅲ Results and Discussion

A. Potentiodynamic Polarization Curves

Figure 1 presents the potentiodynamic polarization curves of 6005A aluminum alloy after passivation for different durations. As shown in the figure, the passivation time exerts a significant influence on the corrosion resistance of the alloy, exhibiting a clear trend of “initial improvement followed by degradation.”

As the passivation time increased from 10 min to 70 min, the corrosion resistance of the specimens gradually improved. At 70 min, the alloy exhibited the best corrosion protection performance, characterized by the lowest corrosion current density and the most positive pitting potential. However, when the passivation time was further extended to 90 min, a noticeable deterioration in corrosion resistance occurred.

These results indicate that, under the experimental conditions of this study, a passivation duration of 70 minutes provides the optimal process time for forming a highly protective passive film on the 6005A aluminum alloy surface. A detailed analysis of the corresponding electrochemical parameters is discussed below.

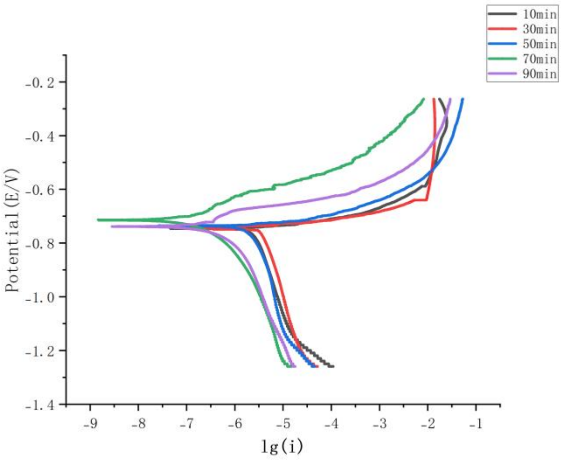

By fitting the polarization curves using the Tafel extrapolation method, the corresponding electrochemical parameters — including the corrosion potential (E_corr), corrosion current density (I_corr), and pitting potential (E_b) — were obtained. The detailed results are summarized in Table 1.

T/min	I_{corr}/(A/cm^2)	E_{corr}/V	E_b/V	$\Delta E/V$	β_A/(V/dec)	β_C/(V/dec)
10	3.96004×10^{-6}	-0.84330	-0.58262	0.26068	13.70812	-2.09381
30	4.93628×10^{-6}	-0.81170	-0.63853	0.17317	17.34323	-2.03100
50	2.68732×10^{-6}	-0.76240	-0.48318	0.27922	18.04629	-2.37284
70	9.17001×10^{-8}	-0.69299	-0.38147	0.31152	20.08064	-7.02770
90	2.85102×10^{-7}	-0.69896	-0.48772	0.21124	41.34962	-4.71025

From a thermodynamic perspective, a more positive corrosion potential (E_corr) indicates a lower tendency for the material to corrode. From a kinetic viewpoint, a smaller corrosion current density (I_corr) corresponds to a slower corrosion rate, reflecting better corrosion resistance.

As shown in Table 1, for all passivation durations, the absolute value of the anodic Tafel slope (β_a) is greater than that of the cathodic Tafel slope (β_c), indicating that the corrosion rate of the 6005A aluminum alloy is primarily controlled by the anodic dissolution process.

With increasing passivation time, the overall E_corr values gradually shift in the positive direction and reach the most positive value of –0.69299 V at 70 min, suggesting a reduced corrosion tendency. Meanwhile, the I_corr values decrease significantly with longer passivation time, reaching a minimum of 9.17×10^{-6} A/cm^2 at 70 min — one to two orders of magnitude lower than that of other samples. This clearly demonstrates that the passivation film formed after 70 min is the most compact and uniform, providing optimal protection for the alloy substrate.

However, when the passivation time is further extended to 90 min, E_corr slightly shifts in the negative direction, and I_corr increases to 2.85×10^{-5} A/cm^2, indicating a decline in corrosion resistance. This degradation may result from the excessive passivation time, during which the acidic solution partially dissolves or damages the previously formed film, reducing its protective effectiveness.

The pitting potential (E_b) serves as a key indicator of a material’s resistance to localized corrosion — the more positive the value, the stronger the pitting resistance. The passivation range (ΔE = E_b – E_corr) reflects the stability of the passive film; a wider ΔE implies a more stable film. According to the data in Table 1, the specimen passivated for 70 min exhibits the most positive E_b (–0.38147 V) and the widest passivation range (0.31152 V).

In summary, the corrosion resistance of the 6005A aluminum alloy does not improve indefinitely with prolonged passivation time. There exists an optimal passivation duration — under the present experimental conditions, 70 minutes yields the best overall corrosion performance.

B. Electrochemical Impedance Spectroscopy (EIS)

Figure 2 presents the electrochemical impedance spectroscopy (EIS) results of the 6005A aluminum alloy after passivation for different durations, measured in a 3.5% NaCl solution. Figure 2(a) shows the corresponding Nyquist plots, while Figure 2(b) illustrates the Bode plots.

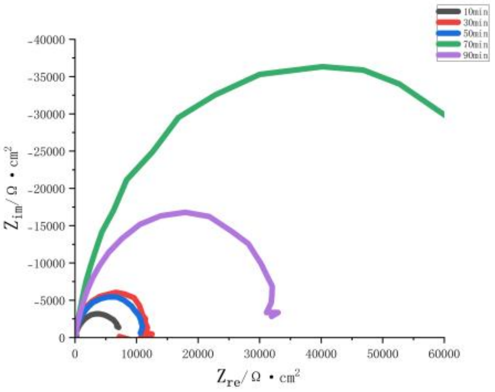

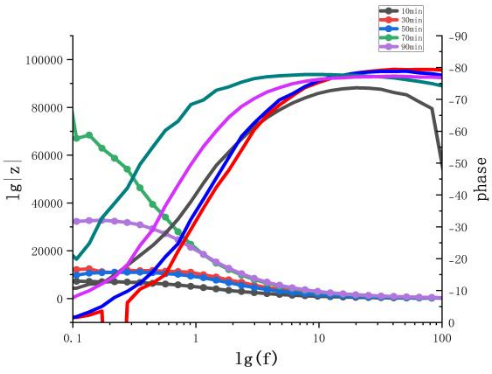

1) Analysis of Nyquist Plots

As shown in Figure 2(a), all specimens subjected to different passivation times exhibit impedance spectra characterized by a single capacitive arc, which appears as a slightly depressed semicircle. This indicates that the electrochemical behavior at the electrode/solution interface during corrosion is governed by a single time constant, typically associated with the charge transfer process and the electric double layer.

The radius of the capacitive arc directly reflects the resistance to charge transfer across the metal–solution interface, serving as a key indicator of the corrosion resistance of the material. A larger arc radius corresponds to a higher charge transfer resistance and, consequently, better corrosion resistance.

By comparing the radii of the capacitive arcs for different passivation durations, the following order can be observed: 70 min > 50 min > 30 min > 90 min > 10 min. Within the range of 10 to 70 minutes, the arc radius increases significantly with passivation time, indicating that the quality and protective performance of the passive film continuously improve during this period. At 70 minutes, the arc radius reaches its maximum value, suggesting the formation of the most protective and compact passive film. However, when the passivation time is further extended to 90 minutes, the arc radius decreases sharply — even smaller than that at 30 minutes — implying deterioration of the passive film due to over-passivation. This trend is consistent with the results obtained from the potentiodynamic polarization analysis.

2) Analysis of Bode Plots

The Bode plots shown in Figure 2(b) provide more detailed information regarding the frequency response characteristics of the system. In the Bode magnitude plots (log|Z| vs. log(f)), the impedance modulus |Z| at low frequencies generally corresponds to the total polarization resistance, which can be used to evaluate the corrosion resistance of the material. As observed from the figure, at the low-frequency region around 10^{-2} Hz, the order of |Z| values is entirely consistent with that of the capacitive arc radii in the Nyquist plots. The specimen passivated for 70 minutes exhibits the highest low-frequency impedance modulus, further confirming its superior corrosion resistance.

In the Bode phase angle plots (Phase vs. log(f)), all curves display a single distinct peak, which supports the conclusion that the corrosion process is governed by a single time constant. The closer the peak phase angle approaches −90°, the more ideally capacitive the electrode surface becomes, indicating a more uniform and compact passive film. The 70-minute specimen shows the largest phase angle peak with the broadest peak width, signifying the formation of the most homogeneous and defect-free passive film among all tested samples.

Ⅳ. Conclusion

The chemical passivation time is a critical process parameter affecting the corrosion resistance of 6005A aluminum alloy. When passivated in 1 mol/L H_2SO_4 solution at room temperature (25 ± 2°C), the corrosion resistance of the alloy exhibits a trend of *initial enhancement followed by deterioration* with increasing passivation time. The specimen passivated for 70 minutes forms the most effective chemical conversion film, providing the strongest corrosion protection. However, when the passivation time is extended to 90 minutes, the protective performance of the film degrades significantly, leading to a noticeable decline in corrosion resistance.

Electrochemical measurements confirm that 70 minutes is the optimal passivation duration. The potentiodynamic polarization (PDP) analysis indicates that the corrosion process of 6005A aluminum alloy is mainly controlled by the anodic dissolution reaction. After 70 minutes of passivation, the specimen exhibits the most positive corrosion potential (E_corr = −0.69299 V) and pitting potential (E_b = −0.38147 V), together with the lowest corrosion current density (I_corr = 9.17001×10^{-8} A/cm²) and the widest passivation interval (ΔE = 0.31152 V).

The electrochemical impedance spectroscopy (EIS) results are highly consistent with the polarization data. All Nyquist plots exhibit a single capacitive arc, indicating that the corrosion process is dominated by charge transfer control. The sample passivated for 70 minutes shows the largest capacitive arc radius, the highest low-frequency impedance modulus, and the widest and most intense phase angle peak in the Bode plots. These features collectively demonstrate that the passive film formed after 70 minutes of passivation is the most compact, uniform, and stable, providing the most effective corrosion protection for the 6005A aluminum alloy substrate.

Ⅴ.Reference

[1] X. Luo, T. Wang, X. Sun et al., “Effect of test parameters on intergranular corrosion test results of 5083-H116 aluminum alloy,” Physico-Chemical Inspection - Physical Testing, vol. 61, no. 9, pp. 7–11, 2025. DOI: CNKI:SUN:LHJW.0.2025-09-002.

[2] D. Xia, C. Pan, Y. Guo et al., “EIS study on interfacial states and corrosion mechanisms of 7050 aluminum alloy under cavitation in NaCl solution,” Journal of Chinese Society for Corrosion and Protection, vol. 45, no. 5, pp. 1196–1204, 2025. DOI: CNKI:SUN:ZGFF.0.2025-05-005.

[3] H. Zhang, P. Jia, and D. Du, “Research on hard anodizing process and salt spray corrosion resistance of ultra-high-strength aluminum alloy,” Equipment Environmental Engineering, vol. 22, no. 8, pp. 14–23, 2025. DOI: CNKI:SUN:JSCX.0.2025-08-002.

[4] C. Xiong, Z. Guo, Y. Zhang et al., “Study on corrosion and conductivity performance of CrN and CrCN coatings on aluminum bipolar plates for PEMFC,” Modern Transportation and Metallurgical Materials, vol. 5, no. 4, pp. 17–24, 2025. DOI: CNKI:SUN:YAJI.0.2025-04-003.

[5] Z. Ding, S. Zhang, X. Xiao et al., “Intergranular corrosion behavior of semi-solid 7075 aluminum alloy friction stir welded joints,” Journal of Chinese Society for Corrosion and Protection, vol. 45, no. 4, pp. 1089–1097, 2025. DOI: CNKI:SUN:ZGFF.0.2025-04-018.

[6] T. Wen, “Effect of shot peening surface strengthening on corrosion resistance of 6061-T6 aluminum alloy,” M.S. thesis, Anhui University of Science and Technology, 2025. DOI: 10.26918/d.cnki.ghngc.2025.001001.

[7] J. Cheng, D. Huang, H. Huang et al., “Study on the performance of a shielding-type anti-corrosion coating suitable for aluminum alloy surface,” China Coatings, vol. 40, no. 5, pp. 35–40, 2025. DOI: 10.13531/j.cnki.china.coatings.2025.05.005.

[8] Z. Huang, G. Liu, W. Fan et al., “Effect of passivation time on corrosion resistance of 304 stainless steel,” Journal of Chinese Society for Corrosion and Protection [Online], pp. 1–12, 2025. [Accessed: Oct. 14, 2025]. Available: https://link.cnki.net/urlid/21.1474.TG.20250527.1350.010

[9] Q. Huang, “Study on Zn-Ni alloy electroplating and Cr black passivation process of 2024 aluminum alloy,” M.S. thesis, Guizhou Normal University, 2025. DOI: 10.27048/d.cnki.ggzsu.2025.001760.

[10] C. Li, A. Wang, X. Zhu et al., Corrosion and Chemical Passivation Technology of Aluminum, Beijing: Chemical Industry Press, 2024, p. 280.

[11] Y. Ji, X. Wang, D. Xia et al., “Passivation film corrosion resistance of 1060, 2024 and 5083 aluminum alloys: EIS, XPS and first-principles calculation,” in Proc. 9th Marine Materials and Corrosion Protection Conf. & 3rd Durability and Safety of Reinforced Concrete Facilities Conf., Tianjin Univ. & Northwestern Polytechnical Univ., 2023, pp. 59. DOI: 10.26914/c.cnkihy.2023.041336.

[12] B. Guo, “Development and performance study of trivalent chromium passivation solution for 2024 aluminum alloy,” M.S. thesis, Institute of Mechanical Science Research, 2022. DOI: 10.27161/d.cnki.gshcs.2022.000035.

[13] Y. Wu, “Study on corrosion resistance and mechanical properties of 2024 aluminum alloy,” M.S. thesis, Ningxia University, 2022. DOI: 10.27257/d.cnki.gnxhc.2022.000458.

[14] E. Chen and L. Dang, “Passivation process and corrosion resistance of passivation film on 5052 aluminum alloy,” Materials Protection, vol. 55, no. 1, pp. 142–146, 2022. DOI: 10.16577/j.issn.1001-1560.2022.0018.

[15] Y. Ren, D. Li, C. Liu et al., “Comparative study of Ti/Zr passivation and Cr passivation performance of 6063 aluminum alloy,” Aluminum Processing, no. 4, pp. 19–21+26, 2021. DOI: CNKI:SUN:LJGO.0.2021-04-014.

[16] X. Ye, “Study on self-crosslinked acrylic resin passivation film on aluminum alloy surface,” M.S. thesis, Anhui University of Technology, 2020. DOI: 10.27790/d.cnki.gahgy.2020.000485.

[17] H. Hu, “Experimental design on corrosion resistance of organic–inorganic composite chromium-free passivation film for aluminum alloy,” China Metal Bulletin, no. 4, pp. 102–103, 2020. DOI: CNKI:SUN:JSTB.0.2020-04-054.

[18] N. Li, C. Dong, and C. Man et al., “Effect of intermetallic compounds on pitting behavior and passivation film structure of aluminum alloy surface,” in Proc. 10th National Corrosion Conference Abstracts, Beijing Institute of New Materials Technology, 2019, pp. 312. DOI: 10.26914/c.cnkihy.2019.015898.

[19] D. Li, S. Zhang, and P. Yan, “Study on chromium-free passivation of aluminum alloy surface,” Electroplating and Environmental Protection, vol. 38, no. 3, pp. 34–36, 2018. DOI: CNKI:SUN:DDHB.0.2018-03-016.

[20] S. Cui, “Study on chromium-free passivation process and properties of aluminum and aluminu

[21] H. Xia, Z. Mao, and D. Zhang, “Preparation and performance of high-corrosion-resistant composite passivation film for aluminum alloy,” Materials Protection, vol. 49, no. 7, pp. 52–55+7, 2016. DOI: 10.16577/j.cnki.42-1215/tb.2016.07.015.

[22] S. Chen, “Study on preparation process and corrosion resistance of rare earth passivation film on ADC12 aluminum alloy,” M.S. thesis, Chongqing University, 2016.

[23] C. Feng, Y. Huang, and Y. Shen et al., “Effect of different surface states on corrosion resistance of 6061 aluminum alloy,” Equipment Environmental Engineering, vol. 12, no. 4, pp. 100–104+128, 2015. DOI: CNKI:SUN:JSCX.0.2015-04-021.

[24] J. Hou, “Effect of passivation time on morphology and corrosion resistance of rare earth conversion film on aluminum alloy,” Guangdong Science and Technology, vol. 24, no. 6, pp. 52–53, 2015. DOI: CNKI:SUN:GDKJ.0.2015-06-020.

[25] B. Hu, “Corrosion behavior of 7075 aluminum alloy in alkaline NaCl medium and inhibition effect of rare earth passivation,” M.S. thesis, Qinghai Normal University, 2014.

[26] D. Veys-Renaux, N. Chahboun, and E. Rocca, "Anodizing of multiphase aluminium alloys in sulfuric acid: in-situ electrochemical behaviour and oxide properties," Electrochim. Acta, vol. 211, pp. 1056–1066, Sep. 2016, doi: 10.1016/j.electacta.2016.06.131.

[27] W. Xue, Y. Wang, Z. Chen, and C. Dong, "Effect of oxidation time on microstructure and corrosion properties of micro-arc oxidation coatings on 6061 aluminum alloy," Materials Protection, vol. 46, no. 11, pp. 1-4, Nov. 2013.